

A STUDY OF SPATIAL AND TEMPORAL DISTRIBUTION OF MARTIAN POLAR COLD SPOTS. C. Cornwall¹ and T. N. Titus², ¹Department of Geology, Northern Arizona University, Flagstaff, Arizona, ²United States Geological Survey, Flagstaff, Arizona.

Introduction: Approximately one-quarter of the Mars atmosphere is cycled through the seasonal ice caps each year [1,2]. This CO₂ cycle, which is the dominant driver of the global climate of Mars, is a balance of energy input (solar insolation) and radiative losses to space. The physical properties of the CO₂ ice (e.g. grain size, dust content) can affect the energy balance by changing the amount of solar insolation absorbed or the amount of thermal energy radiated to space [3].

In the 1970s, Mariner and Viking observations of the polar regions of Mars revealed winter brightness temperatures that were considerably below the expected kinetic temperatures for CO₂ ice sublimation [4]. Three early hypotheses suggested that these cold spots were (1) high-altitude CO₂ clouds [5], (2) surface CO₂ with low emissivity [6], and low-kinetic surface temperatures due to lower-than-expected CO₂ partial pressures [7]. Analysis of Mars Global Surveyor (MGS) Thermal Emission Spectrometer (TES) data [8, 9] and Mars Orbiter Laser Altimeter (MOLA) data [8,10] suggest that most of the cold spots are surface emissivity effects from fine-grained CO₂ snow. A few of the “coldest” cold spots are probably CO₂ blizzards in progress [8].

Data: This study uses MGS TES data over a period of three Mars years. We utilize 2 subsets of the TES polar data: (1) the polar ring (Latitude 86-87.2) and (2) “cold spot only” data, where only the observations with bolometer brightness temperatures less than 135 K are used.

The polar ring data, while limited to a small latitude range, is convenient to constrain the sizes and lifetimes of cold spots due to the high-frequency of repeat coverage. The “cold spot only” data is beneficial to evaluate seasonal and spatial distributions of cold spots.

Cold spots are identified by drops in the 25 μm emissivity, which translate into lower 25 μm brightness temperatures. For this study, we use the convention of Titus et al. [8], defining a cold spot index of brightness temperature differences between 18 μm and 25 μm ($T_{18}-T_{25}$).

Analysis Techniques: Data from the TES database provides a way to study spatial and temporal values of cold spots. Spatial and temporal fits of the TES cold spot observations ($T_{18}-T_{25}$) are obtained by using a two dimensional Gaussian convolved with an exponential decay. These fits provide estimates for both

size (1-sigma) and intensity of the cold spot (amplitude).

Results:

Northern cold spots within the polar ring. In the northern polar ring, 68% of all cold spots occurred in late winter, after L_s 300°. Cold Spots independent from topography typically formed earlier in the autumn than cold spots that were linked to topography. On the perennial cap, cold spots generally occurred on or near slopes and scarps, where the topographic relief induced orographic lifting. Cold spots that occurred in clusters were generally less intense (amplitudes ~ 21° Celsius) when compared with cold spots that were isolated (amplitudes ~ 26° Celsius). Areas of intense activity, where numerous cold spots formed and were indistinguishable from each other, were often linked to topographic features. Cold spots associated with topography were generally smaller, averaging in radius (1-Sigma) ~ 57km. Cold spots not associated with topography averaged ~82km in radius. In general, most North Polar Ring cold spots had amplitudes of approximately 24° Celsius to form and were usually larger than those found in the South Polar Ring. Cold spot size in the north varied with season, decreasing as winter solstice approached, then increasing again in mid winter. Average half-lives for the majority of cold spots in the north lasted about 4° of L_s and shorter. Half-lives closely correlated to season as well, increasing during mid autumn, then decreasing during winter solstice, and increasing again in mid winter.

Southern cold spots within the polar ring. In the south polar ring, 45% of all cold spots occurred during the winter. The majority of cold spot activity in the south occurred before winter solstice around L_s 82°. Cold spots were restricted to the location of the perennial cap. Clustered cold spot activity generally occurred with an average amplitude of 20° Celsius as opposed to isolated cold spots, which had an average amplitude of 25° Celsius. The South Polar Ring did not display any episodes of intense cold spot activity over a period of three Mars years. Topography related cold spots had an average size (sigma) of 46km with amplitude of 17° Celsius and cold spots independent of topography averaged a size (sigma) of 50km with an amplitude of 22° Celsius. Average half-lives for cold spots in the south were similar to those found in the north, but in the south, half-lives were more dependent

upon the size of the cold spot. A larger cold spot in the south had a longer half-life.

Cold spot only data in the north. The majority of northern cold spots occurred during the polar night. (See Fig 1.) Outside the polar night, they occurred in the autumn more than in the winter, and most of these cold spots formed independently from topographic features.

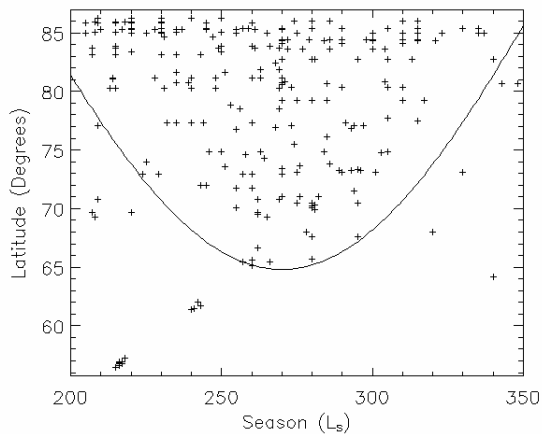


Figure 1: MY 24 cold spot formation as a function of latitude vs. season. The line represents the edge of polar night.

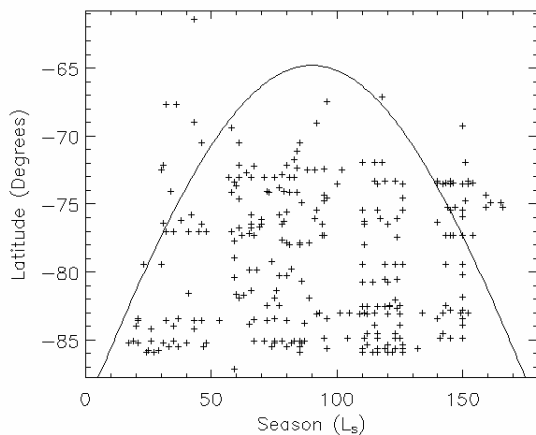


Figure 2: MY 26 cold spot formation as a function of latitude vs. season. The line represents the edge of polar night.

Cold spot only data in the south. Cold spot distributions in the south were similar to those in the north. Most cold spots formed within the polar night, but there were exceptions (Fig. 2). More southern cold spots formed outside the polar night during the winter season, which is opposite from the behavior observed in the north. Almost all of the cold spots that formed

outside polar night were associated with topography, primarily cratered terrain.

Effects from the global dust storm. The global dust storm occurred between L_s 180° and 270° (Mars year 25) and affected cold spot activity on the North Polar Ring by modifying the seasonal distribution of both topographically dependent and independent cold spots. During the dust storm, there was a decrease in cold spot activity for cold spots associated with topography and an increase for cold spots not associated with topography. After the storm died, topographically based cold spot activity increased to twice that of the previous year. The effects from the global dust storm were less severe in the South Polar Ring because the dust storm did not occur during the autumn and winter seasons for the southern hemisphere. In the southern autumn season following the dust storm, the South Polar Ring had a slight increase in topography based cold spot activity and a decrease in topography independent cold spots.

The effects of the global dust storm in the north would suggest that the lack of planetary insolation reduced the available energy needed to form topography based cold spots, resulting in a decrease in activity. Cold spot activity that was independent of topography was probably affected by an injection of dust particles. The dust particles most likely became the nuclei for snow formation.

Significance: The differences found between the North Polar Ring and the South Polar Ring cold spots are indications of the polar atmospheric surface interactions and processes. The global dust storm of Mars year 25 may have increased that amount of high-altitude CO_2 condensation (snow) while inhibiting orographic lifting associated with topographical relief.

References: [1] Tillman, J.E. et al. (1993) *JGR*, **98**, 10963-10971. [2] Kelly, N.J. et al. (2006) *JGR*, **111**, CiteID E03S07. [3] James, P.B. et al. (1992) In *Mars*, 934-968. [4] Kieffer et al. (1976) *Sci.* **193**, 780-786. [5] James et al. 2005 [3] Titus T. N. et al (2001) *JGR*, **106**, 181. [6] Hunt, G.E. (1980) *GRL*, **7**, 481-484. [7] Dittion, R. and Kieffer H.H. (1979) *JGR*, **84**, 8294-8300. [8] Kieffer, H.H. et al. (1977) *JGR*, **82**, 4249-4291. [9] Titus, T.N. et al. (2001) *JGR*, **106**, 23181-23196. [10] Hansen, G. (1997) *JGR*, **104**, 16471-16486. [11] Ivanov, A.B. and Muhleman, D.O. (2001) *Icarus*, **154**, 190-206.